Ionization of the hydrogen atom by intense ultrashort laser pulses

S. Borbély,[1] K. Tőkési,[2] and L. Nagy[1]
[1]*Faculty of Physics, Babeş-Bolyai University, Kogălniceanu Street No. 1, 400084 Cluj, Romania*
[2]*Institute of Nuclear Research of the Hungarian Academy of Sciences (ATOMKI), P.O. Box 51, H-4001 Debrecen, Hungary*
(Received 19 November 2007; revised manuscript received 29 January 2008; published 17 March 2008)

The ionization of atomic hydrogen in intense laser fields is studied theoretically by both quantum-mechanical and classical approaches. In the quantum-mechanical treatment we apply a momentum-space strong-field approximation (MSSFA) and the Coulomb potential is taken into account as a perturbation. The classical calculations are performed within the framework of the classical trajectory Monte Carlo method. The energy and angular distributions of the ionization probabilities of the photoelectrons are presented for different laser pulses. While for the case of low electron energies larger discrepancies can be observed between the theories in the double-differential ionization probabilities, at high electron energies the agreement is excellent. This indicates that the generation of low-energy electrons is of quantum type and it is strongly influenced by the Coulomb potential, while the production of high-energy electrons is of classical type and it is less influenced by the Coulomb interaction. Our MSSFA results are in good agreement with the most reliable calculations based on a numerical solution of the time-dependent Schrödinger equation for high momentum transfers.

DOI: 10.1103/PhysRevA.77.033412 PACS number(s): 32.80.Rm, 32.80.Fb, 42.50.Hz

I. INTRODUCTION

In the last years advanced laser facilities have achieved intensities of the order of 10^{15} W/cm^2 and pulse lengths of the order of 10 fs, which corresponds to few cycles of an electrical field of 800 nm wavelength [1–3]. In the past years research activities have turned to investigations of the interactions between such short and strong pulses with matter.

In the multiphoton regime, many experimental [4–8] and theoretical studies [9–14] have been performed. In the tunneling regime, on the other hand, recent experiments [15,16] with linearly polarized lasers have shown structures in the momentum distribution of the photoionized electrons in rare gases which have not been fully understood so far. The role of interference in few-cycle pulses is also investigated both theoretically and experimentally [17–19].

These processes are of considerable interest for basic and applied science. From the fundamental point of view they might broaden our general understanding of the dynamics of atomic processes for laser-matter interactions and field-free collisions. These studies can help us to find the way for the control of ultrashort quantum processes which are important in a number of applications, like in laser-driven fusion, in plasma heating, or in the development of fast optical electronic devices. The dynamics of atomic processes for the above-mentioned interactions are not fully understood due to the lack of the exact and efficient theoretical models. For a detailed understanding of processes involved in the laser-matter interaction one needs to solve the time-dependent Schrödinger equation (TDSE) for an atomic system in the radiation field, but its exact analytical solution is not known. Several numerical solutions of the Schrödinger equation for these kinds of systems are known [20–26], but they are very time consuming for large systems and converge slowly at high radiation intensities. To overcome this problem there are several theoretical approaches, which are based on the simplification of the TDSE using different approximations depending on the laser field parameters.

At low-and moderate laser field intensities the time-dependent perturbation theory (TDPT) is a well-known approximation for single-photon and multiphoton processes and even for above-threshold ionization [9]. In this case the TDSE is solved by considering the interaction between the laser field and the studied atomic system as a perturbation. The TDPT approach breaks down at higher laser intensities when it fails to describe the "peak suppression" in the above-threshold ionization spectra [27,28].

At higher laser field intensities other nonperturbative processes emerge, like high-harmonics generation, tunneling ionization (TI), and over-the-barrier ionization (OBI), which cannot be described using TDPT and other approaches are necessary.

The most frequently used models are based on the Keldysh theory [29,30]. The Keldysh theory is based on the assumption that on the final-state wave function only the external laser field has a dominant influence and it can be considered as a momentum eigenstate. The main shortcoming of the Keldysh theory is that it completely neglects the long-ranged Coulomb interaction between the ionized electron and remaining target ion. The Coulomb interaction leads to phenomena like subpeaks in the above-threshold ionization spectra [31] and asymmetry in the spatial distribution of the ejected electrons even for symmetric few-cycle laser pulses [32], which cannot be explained in the simplified Keldysh formalism. There are two possible ways of including the Coulomb interaction in the Keldysh formalism. The first one is by making corrections in the transition matrix, and the second one is by making corrections in the Volkov wave function [33]. Approaches based on the Keldysh theory using these corrections have been applied with considerable success to study multiphoton and tunneling ionization of atomic systems [30,34].

In recent years the Coulomb-Volkov wave functions were used to describe processes in the presence of intense ultrashort laser fields [35–38]. The Coulomb-Volkov wave functions were introduced by Jain and Tzoar in 1978 [39] to describe laser-assisted collisions. Later they were success-

fully applied to describe multiphoton and above-threshold ionization [38,40]. The Coulomb-Volkov wave functions are also used to study ionization in tunneling and in the over-the-barrier regime in the framework of the sudden approximation [35,36]. In this work this approach will be called the Coulomb-Volkov (CV) model.

The accuracy of the results provided by the CV model is limited by the sudden approximation (it provides accurate results only if the pulse duration is less then two orbital periods of the active electron [36]) and by the fact that the CV wave functions are only an approximate solution of the TDSE for charged particles in the presence of external radiation fields. From these two main limitations the first one is more restrictive, because it is limited to a pulse duration in the attosecond region. Our goal is to construct a theoretical model, which provides results as good as, or better than, the CV model, but without any limitation in pulse duration.

Our approach is based on the approximate solution of the TDSE for quantum systems with one active electron, where the Coulomb interaction between the electron and the remaining target ion can be considered as a perturbation during the external laser pulse. The time-dependent wave function of the active electron is expanded in terms of Volkov wave functions. The equation for the expansion coefficients obtained from the TDSE is solved iteratively in momentum space. This approach is closely related to the strong-field approximation (SFA) [14]. The main difference between our method and the SFA is that we perform our calculations in momentum space. Therefore, to distinguish our scheme from the traditional SFA, we call our present approach the momentum-space strong-field approximation (MSSFA).

The ionization process in the over-the-barrier regime is considered to be a classical one, and it is believed that it can be described well by classical models like the classical trajectory Monte Carlo (CTMC) [24,36,41] method.

We present double-differential ionization probability densities using the MSSFA, CTMC, and Volkov models for different laser pulses. The ionization probability densities are presented as a function of the electron energy and ejection angle of the ionized electron.

The effect of the Coulomb interaction on the ionization of the hydrogen atom by ultrashort laser pulses using different field intensities and different approaches is investigated in several works [42,43]. In these cases the effect of the Coulomb potential is studied by different descriptions of the final state, like the Coulomb-Volkov wave function [43] or first- and second-order Coulomb-corrected Volkov wave functions, or by employing Coulomb corrections to the Keldysh-Faisal-Reiss theory [42].

In the present paper we also study the effect of the Coulomb potential during and after the laser pulse by analyzing the angular distribution of the electrons at given energies and the ionization probability density (calculated from the double-differential ionization probability density by integration over the ejection angles) using various models.

Atomic units are used throughout the calculations.

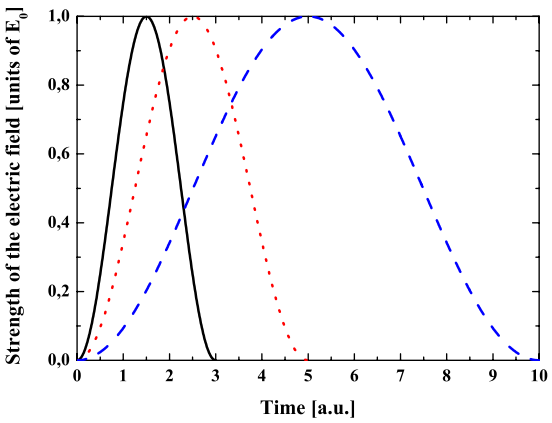

FIG. 1. (Color online) The strength of the laser pulses with $\omega = 0.05$ a.u. used in our calculations for different pulse durations. Solid line: $\tau = 3$ a.u. Dotted line: $\tau = 5$ a.u. Dashed line: $\tau = 10$ a.u.

II. THEORY

A. Characterization of the model

The time evolution of atomic systems in the presence of one intense ultrashort laser pulse is investigated. The laser pulse is defined by its electric component

$$\vec{E} = \begin{cases} \hat{\varepsilon} E_0 \sin(\omega t + \phi_0) \sin^2\left(\frac{\pi t}{\tau}\right) & \text{if } t \in [0, \tau], \\ 0 & \text{otherwise}, \end{cases} \tag{1}$$

where $\hat{\varepsilon}$ is the polarization vector, ω is the frequency of the carrier wave, ϕ_0 is the carrier envelope phase, and τ is the pulse duration. The carrier envelope phase is set as follows:

$$\phi_0 = -\frac{\omega\tau}{2} - \frac{\pi}{2}. \tag{2}$$

Figure 1 shows the shape of the laser pulses used in our calculations.

In the time evolution of the studied system one may distinguish three main time intervals. In the first time interval ($t < 0$) the laser field is not yet switched on and the studied system is in a field free eigenstate. The Hamilton operator of the system in these conditions is

$$\hat{H}_I = \frac{\hat{p}^2}{2} + V(\vec{r}), \tag{3}$$

where $V(\vec{r})$ is the Coulomb potential between the active electron and the rest of the system. The eigenvectors and eigenfunctions of this Hamilton operator are considered to be known, and the initial state of our system coincides with eigenstate ψ_i. Under these conditions the time-dependent wave function of the system is

$$\Psi_I(t) = \psi_i e^{-iE_i t}. \tag{4}$$

During the second time interval ($0 \le t \le \tau$) the laser field is switched on and the Hamilton operator of the system becomes

$$\hat{H}_{II} = \frac{\hat{p}^2}{2} + \vec{r}\cdot\vec{E} + V(\vec{r}), \tag{5}$$

where $\vec{r}\cdot\vec{E}$ is the interaction term between the laser field and the active electron expressed in length gauge. The dipole approximation was implicitly applied when the spatial dependence of $\vec{E}$ was neglected in Eq. (1). The time-dependent Schrödinger equation

$$i\frac{\partial}{\partial t}\Psi_{II}(t) = \hat{H}_{II}\Psi_{II}(t), \tag{6}$$

$\Psi_{II}(t)$ being the wave function of the active electron in the presence of the laser pulse, does not have a known analytical solution. In order to determine the time evolution of the studied system one needs to know the $\Psi_{II}(t)$ wave function. In the present approach the wave function is considered in the form

$$\Psi_{II}(t) = \int d\vec{k}\, c(\vec{k},t)\Psi_V(\vec{k},t), \tag{7}$$

where $\Psi_V(\vec{k},t)$ are the Volkov wave functions. The Volkov wave functions are the solutions of the TDSE in the dipole approximation for a charged particle in a radiation field,

$$i\frac{\partial}{\partial t}\Psi_V(\vec{k},t) = \left(\frac{\hat{p}^2}{2} + \vec{r}\cdot\vec{E}\right)\Psi_V(\vec{k},t), \tag{8}$$

and they can be expressed as

$$\Psi_V(\vec{k},t) = \exp\left(-\frac{i}{2}\int_0^t dt'[\vec{k}+\vec{A}(t')]^2\right)e^{i[\vec{k}+\vec{A}(t)]\cdot\vec{r}}, \tag{9}$$

where

$$\vec{A}(t) = -\int_0^t \vec{E}(t')dt' \tag{10}$$

is the vector potential of the electromagnetic field.

The time-dependent wave function is well defined by the expansion coefficients $c(\vec{k},t)$, so for obtaining the time evolution of the system it is enough to calculate these coefficients.

By substituting the time-dependent wave function of Eq. (7) into the TDSE given by Eq. (6) the following can be obtained:

$$i\frac{\partial}{\partial t}\int d\vec{k}\, c(\vec{k},t)\Psi_V(\vec{k},t) = \left(\frac{\hat{p}^2}{2} + V(\vec{r}) + \vec{r}\cdot\vec{E}\right)\int d\vec{k}\, c(\vec{k},t)\Psi_V(\vec{k},t). \tag{11}$$

Using Eq. (8), Eq. (11) is simplified:

$$i\int d\vec{k}\,\Psi_V(\vec{k},t)\frac{\partial}{\partial t}c(\vec{k},t) = \int d\vec{k}\, c(\vec{k},t)V(\vec{r})\Psi_V(\vec{k},t). \tag{12}$$

Equation (12) can be converted into a more favorable form by transforming it into momentum space:

$$\begin{aligned} i\int d\vec{k}\left(\frac{\partial}{\partial t}c(\vec{k},t)\right)&\exp\left(-\frac{i}{2}\int_0^t dt'[\vec{k}+\vec{A}(t')]^2\right)\int d\vec{r}\, e^{i[\vec{k}-\vec{p}+\vec{A}(t)]\cdot\vec{r}} \\ &= \int d\vec{k}\, c(\vec{k},t)\exp\left(-\frac{i}{2}\int_0^t dt'[\vec{k}+\vec{A}(t')]^2\right)\int d\vec{r}\, V(\vec{r})e^{i[\vec{k}-\vec{p}+\vec{A}(t)]\cdot\vec{r}}. \end{aligned} \tag{13}$$

After basic mathematical operations and the substitution $\vec{s} = \vec{k}-\vec{p}+\vec{A}(t)$, this equation becomes

$$\frac{\partial}{\partial t}c(\vec{q},t) = -\frac{i}{(2\pi)^3}\int d\vec{s}\, c(\vec{s}+\vec{q},t)\exp\left(-\frac{i}{2}\int_0^t dt'\,\vec{s}[\vec{s}+2\vec{q}+2\vec{A}(t')]\right)\int \vec{d}r\, V(\vec{r})e^{i\vec{s}\cdot\vec{r}}. \tag{14}$$

We note, however, that Eq. (14) is equivalent with the Schrödinger equation (6). By solving Eq. (14) one obtains directly the time-dependent wave function in momentum space, which carries all information about the studied system. Equation (14) can be solved numerically, but this direct approach needs large computational resources and in several cases it is more advantageous to introduce some approximations. These approximations usually simplify considerably the problem and lead to results with an accuracy comparable to that of the direct numerical solution.

In the third time interval ($t > \tau$) the laser field is switched off and the Hamilton operator of the system can be expressed as

$$\hat{H}_{III} = \frac{\hat{p}^2}{2} + V(\vec{r}), \tag{15}$$

which is identical to the one given in the first time interval.

The time-dependent wave function of the system in this time interval can be given as a linear combination of stationary-state wave functions

$$\Psi_{III}(\vec{r},t) = \sum_b \psi_b e^{-iE_b t} + \int d\vec{k}\, c_f(\vec{k})\psi_f e^{-iE_f t}, \tag{16}$$

where ψ_b represents bound states, while ψ_f represents free states. Wave functions representing free electrons are approximated by plane waves, so we have

$$\psi_f = e^{i\vec{k}\cdot\vec{r}} \tag{17}$$

and

$$E_f = \frac{k^2}{2}. \tag{18}$$

One of the basic properties of the time-dependent wave function which describes the evolution of a real system is that it is continuous over the time. From the continuity condition at time $t=0$ one obtains

$$\psi_i = \int d\vec{k}\, c(\vec{k}, t=0) e^{i\vec{k}\cdot\vec{r}}. \tag{19}$$

From this expression one may get the initial condition for Eq. (14):

$$c(\vec{q}, t=0) = \frac{1}{(2\pi)^3}\langle e^{i\vec{q}\cdot\vec{r}}|\psi_i\rangle. \tag{20}$$

We note that the above initial condition is in fact the initial-state wave function in momentum space, because at $t=0$ the Volkov wave functions are reduced to plane waves. From the continuity condition at $t=\tau$ we get

$$\int d\vec{k}\, c(\vec{k},\tau)\exp\left(-\frac{i}{2}\int_0^\tau dt'[\vec{k}+\vec{A}(t')]^2\right)e^{i\vec{r}\cdot[\vec{k}+\vec{A}(\tau)]}$$
$$= \sum_b \psi_b e^{-iE_b\tau} + \int d\vec{k}\, c_f(\vec{k}) e^{i(\vec{k}\cdot\vec{r}-E_f\tau)}. \tag{21}$$

We are interested in the transition probability to a free final state, which means that we need to know $c_f(\vec{k})$. This can be obtained by transforming Eq. (21) into momentum space and by neglecting the contribution of bound states,

$$c_f(\vec{p}) = c(\vec{p}-\vec{A}(\tau),\tau)e^{-i[E(\vec{p}-\vec{A}(\tau),\tau)-E_f\tau]}, \tag{22}$$

where we used the notation

$$E(\vec{k},T) = \frac{1}{2}\int_0^T dt'[\vec{k}+\vec{A}(t')]^2. \tag{23}$$

The $c_f(\vec{p})$ given by Eq. (22) is the final-state wave function in momentum space.

The transition probability from the initial state ψ_i to a free final state ψ_f, with a well-defined momentum $\vec{p}$, is given as

$$P_{i\to f} = (2\pi)^3|c_f(\vec{p})|^2 = (2\pi)^3|c(\vec{p}-\vec{A}(\tau),\tau)|^2. \tag{24}$$

B. Volkov model as a zeroth-order approximation

The critical point of our model is the solving method of Eq. (14), or in other words, how to propagate our system in the presence of external laser field in the second time interval. The simplest way is by neglecting completely the Coulomb potential $[V(\vec{r})=0]$. This approximation provides good results only for high laser field intensities. In this framework Eq. (14) becomes

$$\frac{\partial}{\partial t}c(\vec{q},t) = 0, \tag{25}$$

which has the following analytical solution using the initial condition (20):

$$c(\vec{q},t) \equiv c^{(0)}(\vec{q}) = \frac{1}{(2\pi)^3}\langle e^{i\vec{q}\cdot\vec{r}}|\psi_i\rangle. \tag{26}$$

From Eq. (22) the final-state wave function in momentum space can be written as

$$c_f(\vec{p}) = c^0[\vec{p}-\vec{A}(\tau)]e^{-i[E(\vec{p}-\vec{A}(\tau),\tau)-E_f\tau]}, \tag{27}$$

which is the initial-state wave function in momentum space shifted by the momentum transfer $\vec{A}(\tau)$ gained from the external laser field.

C. Momentum-space strong-field approximation as a first-order approximation

In most cases, the Volkov model [see Eq. (27)] does not provide accurate results, because the Coulomb interaction at moderate intensities cannot be totally neglected. At moderate laser intensities one can assume that the influence of the Coulomb interaction on the evolution of the system in the second time interval is small and the expansion coefficients $c(\vec{k},t)$ are close to those provided by the Volkov model (27). Based on this argument, Eq. (14) can be simplified by replacing $c(\vec{k},t)$ on the right-hand side by $c^{(0)}(\vec{k})$ as follows:

$$\frac{\partial}{\partial t}c^{(1)}(\vec{q},t) = -\frac{i}{(2\pi)^3}\int d\vec{s}\, c^{(0)}(\vec{s}+\vec{q})\exp\left(-\frac{i}{2}\int_0^t dt'\ \vec{s}[\vec{s}+2\vec{q}+2\vec{A}(t')]\right)\int \vec{dr}\, V(\vec{r})e^{i\vec{s}\cdot\vec{r}}. \tag{28}$$

The same equation can be obtained using a different approach by considering the Coulomb interaction as a small perturbation and by retaining only the first-order terms in $V(\vec{r})$. The advantage of this approximation is that it eliminates the direct coupling between the expansion coefficients $c(\vec{k},t)$, making easier and faster the solution of Eq. (14).

Equation (28) can be simplified and its solution can be given as simple integral

$$c^{(1)}(\vec{q},t) = c^{(0)}(\vec{q}) - \frac{i}{(2\pi)^3}\int_0^t dt'\ I(\vec{q},t'), \tag{29}$$

where

$$I(\vec{q},t) = \int d\vec{s}\, c^{(0)}(\vec{s}+\vec{q})\exp\left(-\frac{i}{2}\int_0^t dt'\ \vec{s}[\vec{s}+2\vec{q}+2\vec{A}(t')]\right)\int \vec{dr}\, V(\vec{r})e^{i\vec{s}\cdot\vec{r}}. \tag{30}$$

Our present approach is similar to the SFA employed Milošević *et al.* [14]. They have approximated the time evolution operator of the system based on the Dyson equation. In their first iteration step the Keldysh-Faisal-Reiss amplitude was obtained, which corresponds to our Volkov amplitude [see Eq. (27)]. In their second iteration step a transition amplitude linear in the Coulomb potential was constructed, which corresponds to our first-order (MSSFA) model. Both approaches are linear in $V(\vec{r})$, but there are several differences between them, which will be analyzed in a future study.

D. Classical trajectory Monte Carlo simulation

The CTMC method has been quite successful in dealing with the ionization process in laser-atom collisions, when,

instead of the charged particles, electromagnetic fields are used for excitation of the target. The CTMC method is a nonperturbative method, where classical equations of motions are solved numerically. A microcanonical ensemble characterizes the initial state of the target. In this work, the initial conditions of the target are taken from this ensemble, which is constrained to an initial binding energy of H($1s$) (0.5 a.u.).

In the present CTMC approach, Newton's classical nonrelativistic equations of motions are solved [44–46] numerically when an external laser field given by Eq. (1) is included. For the given initial parameters, Newton's equations of motion were integrated with respect to time as an independent variable by the standard Runge-Kutta method until the real exit channels are obtained. For the ionization channel the final energy and the scattering angles (polar and azimuth) of the projectile and the ionized electron were recorded. These parameters were calculated at large separation of the ionized electron and the target nucleus, where the Coulomb interaction is negligible.

The single- and double-differential ionization probabilities (P_i) were computed with the following formulas:

$$\frac{dP_i}{dE} = \frac{N_i}{N\,\Delta E}, \tag{31}$$

$$\frac{dP_i}{d\Omega} = \frac{N_i}{N\,\Delta\Omega}, \tag{32}$$

$$\frac{d^2P_i}{dE\,d\Omega} = \frac{N_i}{N\,\Delta E\,\Delta\Omega}. \tag{33}$$

The standard deviation for a differential probabilities is defined through

$$\Delta P_i = P_i\left[\frac{N-N_i}{N-N_i}\right]^{1/2}. \tag{34}$$

In Eqs. (31)–(34), N is the total number of trajectories calculated for the given collision system and N_i is the number of trajectories that satisfy the criteria for the ionization under consideration in the energy interval ΔE and the emission angle interval $\Delta\Omega$ of the electron.

III. IONIZATION OF THE HYDROGEN ATOM

The above-mentioned theoretical approaches are applied to describe the ionization of the hydrogen atom in the over-the-barrier regime. We choose this system because the calculations are relatively easy to perform and because there are several theoretical studies on this system [24,35,36,43].

Using the $1s$ orbital of the hydrogen atom as initial-state wave function,

$$\psi_i = \frac{1}{\sqrt{\pi}}e^{-r}, \tag{35}$$

one obtains the following initial condition for Eq. (14):

$$c^{(0)}(\vec{q}) = \frac{1}{\pi^2\sqrt{\pi}(1+\vec{q}^2)^2}. \tag{36}$$

Using Eq. (36) the ionization probability in the Volkov approximation can be expressed as

$$P_{i\to f}(\vec{p}) = \frac{16}{\pi\{1+[\vec{p}-\vec{A}(\tau)]^2\}^4}. \tag{37}$$

The MSSFA model can also be adapted very easily by using the Coulomb potential

$$V(\vec{r}) = -\frac{1}{r} \tag{38}$$

in Eq. (30), which can be significantly simplified by performing some of the integrals involved:

$$I(\vec{q},t) = \lim_{r_{\max}\to+\infty}\frac{8}{\sqrt{\pi}}\int_0^\infty\int_0^\pi \frac{\sin(\theta_s)d\theta_s ds}{[1+s^2+q^2+2sq\cos(\theta_s)]^2} \times e^{-(i/2)[s^2t+2sq\cos(\theta_s)t+2f(t)s\cos(\theta_s)\cos(\theta_\varepsilon)]}J_0(2sf(t)\sin(\theta_s)\sin(\theta_\varepsilon))[\cos(sr_{\max})-1], \tag{39}$$

where J_0 is a Bessel function of the first kind. The angle between $\vec{s}$ and $\vec{q}$ is θ_s, while the angle between $\hat{\varepsilon}$ and $\vec{q}$ is θ_ε and

$$f(t) = \int_0^t A(t')dt'. \tag{40}$$

By substituting Eq. (39) into Eq. (29) and by performing the remaining integrals numerically we obtained the expansion coefficient in the MSSFA model. From the obtained expansion coefficients the ionization probability is calculated by using Eq. (24).

IV. RESULTS AND DISCUSSION

Calculations are performed using laser pulses with duration τ of 3 a.u., 5 a.u., and 10 a.u. at two different field intensities (E_0=1 a.u. and E_0=10 a.u.). The energy of the photons is ω=0.05 a.u., which is close to the energy of the photons generated by Ti-sapphire lasers. These pulse parameters limits the value of the Keldysh parameter below 0.05, which are characteristic values for the over-the-barrier ionization. The shape of the pulses is shown in Fig. 1.

The double-differential ionization probability densities calculated using the Volkov, MSSFA, and CTMC models are

presented in Fig. 2, where the ionization probability density is plotted as a function of the electron energy and ejection angle. The ejection angle is measured from the polarization vector $\hat{\varepsilon}$, which is in the direction of the z axis. Due to the spherical symmetry of the ground-state wave function and of the Coulomb potential, the double-differential ionization probability has a rotational symmetry, where the rotational axis is in the direction of the polarization vector $\hat{\varepsilon}$ of the laser field. Due to this symmetry, the yOz positive semiplane carries all information about the ionization probability density. At first sight one may observe that at a large scale all three models predict the same probability densities. In each approach the electrons are ejected with maximum probability along the polarization vector $\hat{\varepsilon}$ with energy around the value $\frac{A(\tau)^2}{2}$, which is gained by the momentum transfer $\vec{A}(\tau)$ from the external laser field.

After a detailed analysis, however, important differences can be observed. In the case of the MSSFA and CTMC models the maxima of the predicted probability densities are shifted toward smaller energies. This shift is caused by the Coulomb attraction during the ionization between the active electron and the rest of the system. In a classical picture the ejected electrons are decelerated by the Coulomb attraction.

Other important differences can be identified in the angular distribution of the ejected electrons at fixed energies (W_e), as shown in Fig. 3. The maximum value of each angular distribution is normalized to unity to allow us an easier comparison.

At the low-energy part of the spectrum [see Figs. 3(a) and 3(d), with W_e below the peak observable in Fig. 2], significant differences are observed between the predicted MSSFA and CTMC angular distributions. The observed differences imply a quantum nature of the ionization for low-energy electrons, which cannot be described correctly by classical calculations. These differences start to disappear at higher electron energies [see Figs. 3(b) and 3(e)], where both distributions are roughly the same. However, some minor differences still exist showing a transition between the quantum and classical natures of the ionization. At high energies, the differences observed at lower energies completely disappear [see Figs. 3(e) and 3(f)] and the distributions predicted by the MSSFA and CTMC models are in good agreement, indicating that the ionization mechanism for electrons ejected at high energies behaves classically.

At the low-energy part of the spectrum [see Figs. 3(a) and 3(d)] large discrepancies are also observed between the predicted MSSFA and Volkov angular distributions. These discrepancies show the significant influence of the Coulomb interaction on the ionization of the low-energy electrons. This disagreement between the discussed models diminishes and completely disappears at higher electron energies [see Figs. 3(b), 3(c), 3(e), and 3(f)], which indicates that the Coulomb interaction has less influence on the ionization of the high-energy electrons.

Figure 4 shows the net angular distributions of the ejected electrons obtained from the double-differential probability density by integrating over the electron energies for different pulse durations. The angular distributions predicted by the Volkov and MSSFA models are in good agreement with the CTMC angular distribution, because the contribution of the low-energy electrons in the net angular distribution is negligible, so the influence of the Coulomb potential and the quantum nature of the ionization can also be neglected.

The ionization spectra are calculated from the double-differential ionization probability densities by integrating over the ejection angle. Figure 5 shows the dP/dE probability densities calculated using the MSSFA, Volkov, and CTMC models along with the results of TDSE and CV calculations obtained by Duchateau *et al.* [36]. At high laser field intensity ($E_0=10$ a.u.) very good agreement is observed between the TDSE and CTMC results in Fig. 5(b). At lower laser intensity ($E_0=1$ a.u.) the agreement is acceptable [see Figs. 5(c) and 5(e)], but not as good as in the previous case, because at these intensities tunneling ionization also takes place, which is not considered in our CTMC model. This good agreement between classical and quantum approaches at high laser field intensities was also confirmed by several other studies [24,36], which confirms the classical nature of the over-the-barrier ionization.

The main difference between the Volkov and the MSSFA models is that the Volkov model completely neglects the Coulomb attraction during the ionization process. The effect of the Coulomb interaction on the photoelectrons during the ionization can be studied by comparing the Volkov and MSSFA ionization probability densities. At the high-energy part of each photoelectron spectrum presented in Fig. 5, good agreement can be observed between the Volkov and MSSFA models. The agreement breaks down at small energy values, where the MSSFA spectrum is shifted toward the lower energies. This strong influence of the Coulomb potential on the electrons with low ejection energy was also observed in the angular distribution of ionized electrons and can be explained using a very simple intuitive picture (see Fig. 6). The electrons with high ejection energy have their momentum in the initial state in the same direction as the net momentum transfer. In this way the trajectory of the high-energy electrons leads directly away from the core, with a very small portion close to the core where the Coulomb potential has a significant influence. On the other hand, the electrons with lower ejection energies have a momentum in the initial state, which leads in the opposite direction of the net impulse transfer. In this way the low-energy electrons need to "go around" the core, leading to a trajectory, which has a long portion close to the core, where they can be influenced significantly by the Coulomb interaction.

Results obtained by Duchateau *et al.* [36] using Coulomb-Volkov wave functions and the sudden approximation are also part of our analysis. In the CV model the influence of the Coulomb interaction on the ionization process is not included and it is taken into account only in the final-state wave function.

The accuracy of the MSSFA and CV results is measured by the agreement with the TDSE results considered to be the best. Where TDSE data are not available, those obtained by CTMC calculations are used as reference. At low-intensities for short pulses, the agreement between the CV and CTMC results is better than between the CTMC and MSSFA results [see Fig. 5(c)]. For these pulse parameters the CV model is better, because the net momentum transfer is small, leading

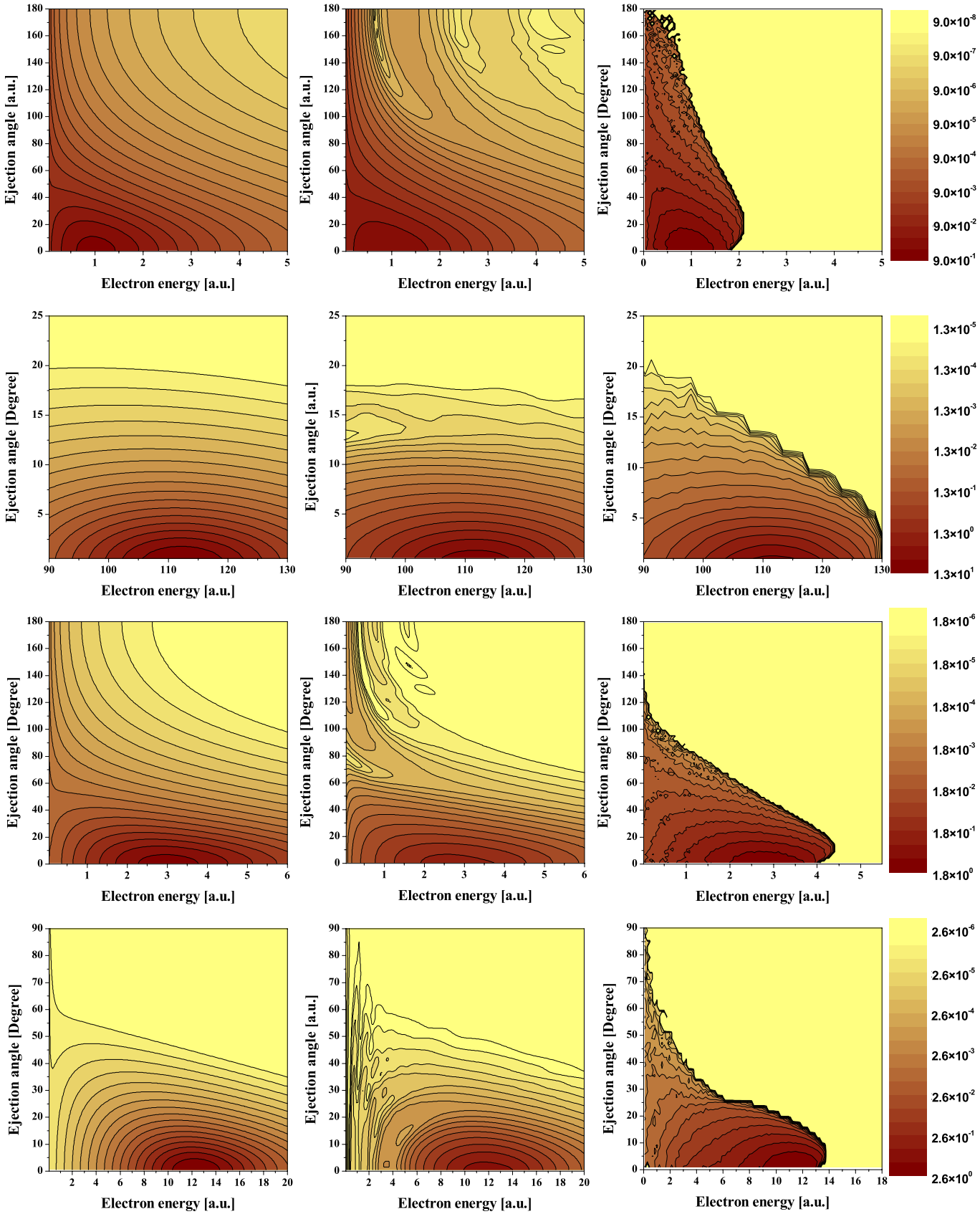

FIG. 2. (Color online) Two-dimensional ionization probability density in the yOz positive semiplane as a function of the electron energy and ejection angle for $\omega=0.05$ a.u. First column: Volkov results. Second column: MSSFA results. Third column: CTMC results. First row: $\tau=3$ a.u. and $E_0=1$ a.u. Second row: $\tau=3$ a.u. and $E_0=10$ a.u. Third row: $\tau=5$ a.u. and $E_0=1$ a.u. Fourth row: $\tau=10$ a.u. and $E_0=1$ a.u.

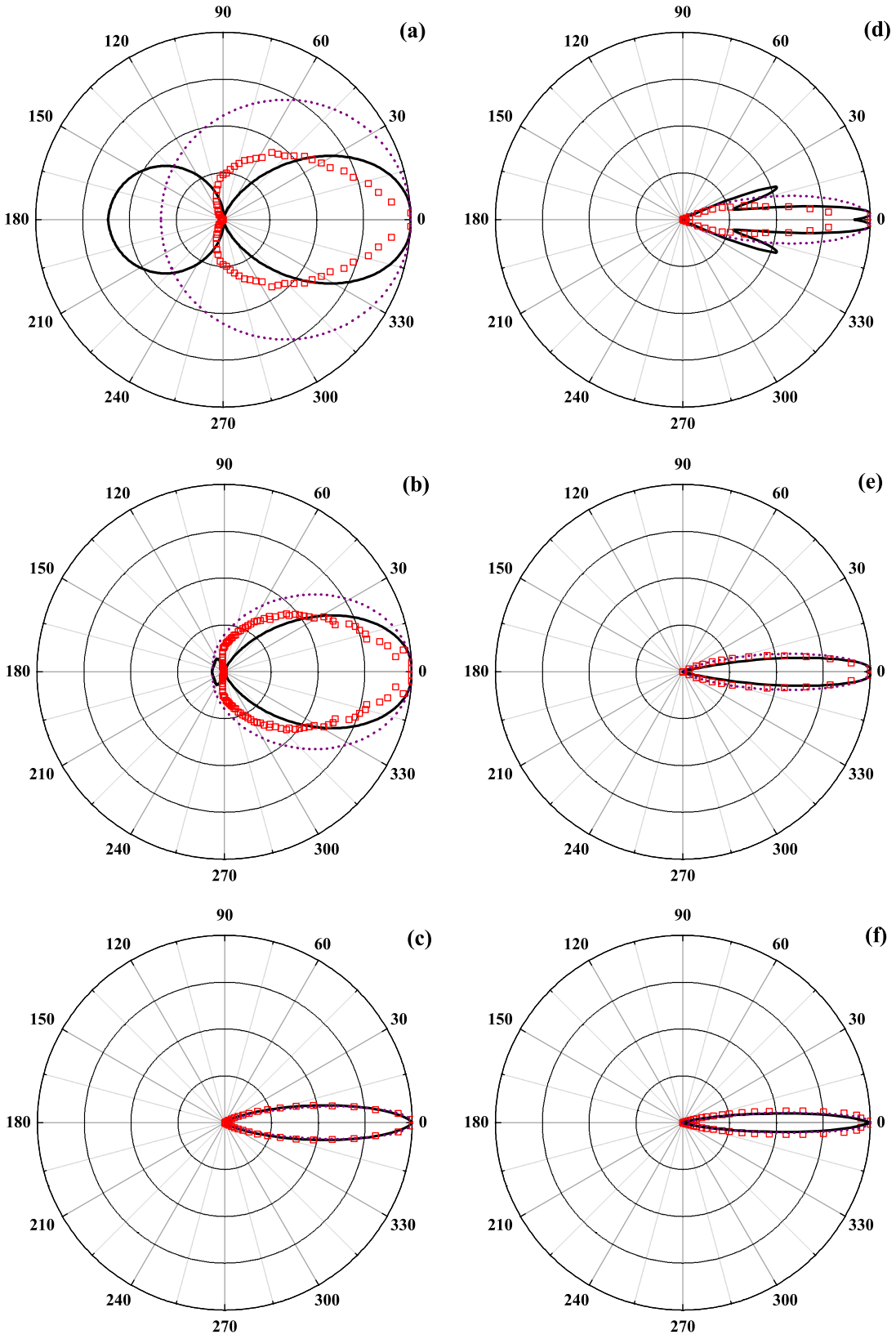

FIG. 3. (Color online) Angular distribution of the photoelectrons for $E_0=1$ a.u., $\omega=0.05$ a.u., and different electron energies (W_e). Solid line: MSSFA. Dotted line: Volkov. Squares: CTMC. First column: $\tau=5$ a.u. Second column: $\tau=10$ a.u. (a) $W_e=0.02$ a.u., (b) $W_e=0.125$ a.u., (c) $W_e=3.5$ a.u., (d) $W_e=4.5$ a.u., (e) $W_e=6$ a.u., and (f) $W_e=10$ a.u.

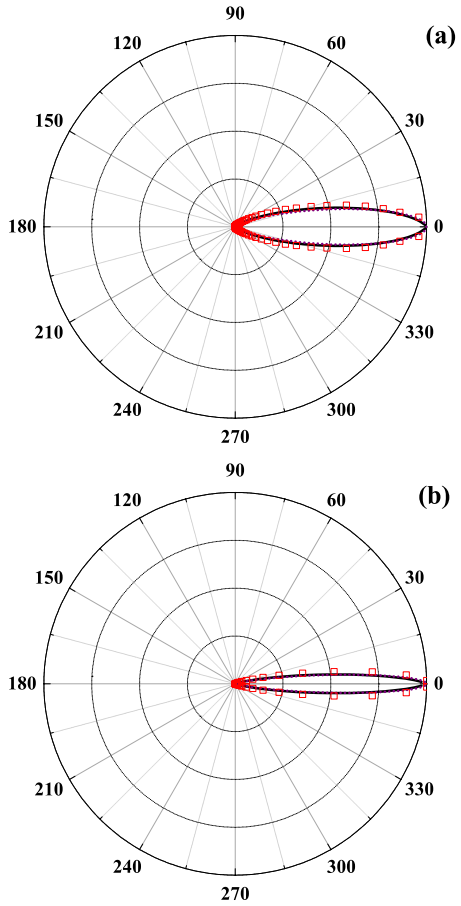

FIG. 4. (Color online) The net angular distribution of the photoelectrons for $E_0=1$ a.u. and $\omega=0.05$ a.u. Solid line: MSSFA. Dotted line: Volkov. Squares: CTMC. (a) $\tau=5$ a.u. and (b) $\tau=10$ a.u.

to photoelectrons with small momentum in the final state, which cannot be described correctly by the plane waves employed in the MSSFA model. At the same intensity but for longer pulses, major discrepancies can be observed between CV and TDSE (CTMC) results [see Fig. 5(e)], because for the longer pulse durations the sudden approximation no longer applies and the Coulomb potential has a visible influence during the ionization process. Discrepancies are also observed between the MSSFA and TDSE (CTMC) results, because the final-state wave function is still inaccurate. At high laser field intensity the agreement between the MSSFA and TDSE results is better than between the CV and TDSE results [see Fig. 5(b)]. In this case the momentum transfer is high, leading to photoelectrons with high energies, where the plane-wave approximation for the final state is accurate. At the low-energy part of the spectra presented in Figs. 5(b), 5(d), and 5(f), the MSSFA results show good agreement with the TDSE (CTMC) results, but discrepancies exist at the high-energy part of the spectra. Here, both the MSSFA and CV models predict higher ionization probabilities than the TDSE (CTMC) model, which in the case of the first-order model can be corrected by taking into account the Coulomb interaction in the final-state wave function.

V. CONCLUSIONS AND OUTLOOK

In the present work a general approach for the ionization of atomic systems by ultrashort laser pulses in one active electron approximation was presented. The time-dependent Schrödinger equation of the system was transformed into momentum space, where it was solved in an iterative way. In the zeroth-order solution the Coulomb potential was neglected and the Volkov model was obtained, while in the first-order solution the Coulomb potential was taken into account during the ionization as a perturbation, leading to the momentum-space strong-field approximation. There are several similarities between the present MSSFA model and the SFA model employed by Milošević *et al.* [14] for above-threshold ionization (ATI). The comparison of theses models in the multiphoton ionization and ATI regime is an interesting subject of a future work.

Calculations were performed for the ionization of the hydrogen atom in the over-the-barrier regime using the Volkov and MSSFA solutions of the time-dependent Schrödinger equation. Classical trajectory Monte Carlo calculations were also performed. The results obtained were analyzed and compared with results obtained by Duchateau and coworkers [36] using the TDSE and CV models.

The double-differential ionization probability densities as a function of the ejection energies and ejection angles were calculated using the Volkov, MSSFA, and CTMC models for different laser pulses. Good agreement was found between the results using these three models at high laser field intensities. This good agreement between classical and quantum calculations was also confirmed by other groups [24,36]. At lower intensities, however, small discrepancies appeared due to the tunneling ionization.

The MSSFA and CTMC results were shifted toward smaller energies due to the Coulomb attraction of the remaining target ion.

More differences were identified by analyzing the angular distribution of the ejected electrons. For low-energy electrons major discrepancies have been found between CTMC and MSSFA results, because the ionization of these low-energy electrons is a quantum process, which cannot be described by a classical approach. At higher electron energies, the observed discrepancies disappear, leading to the conclusion that the ionization process of the high-energy electrons can be described classically. At low energies, differences were also observed between the MSSFA and Volkov results, which disappeared at higher electron energies, indicating that during the ionization electrons with higher energies are less influenced by the Coulomb interaction. The same observation was made by analyzing the ionization spectra, where significant differences between the Volkov and MSSFA results were observed for low-energy photoelectrons. A simple explanation for this behavior was found by considering the possible classical trajectories of the electrons during the ionization. A similar conclusion was also drawn by Zhang and Nakajima [43] in their study, where they found that the influence of the Coulomb interaction depends mainly on the energy of the photoelectrons rather than on the laser field intensities.

The influence of the Coulomb potential during and after the laser pulse was also studied. For short laser pulses with

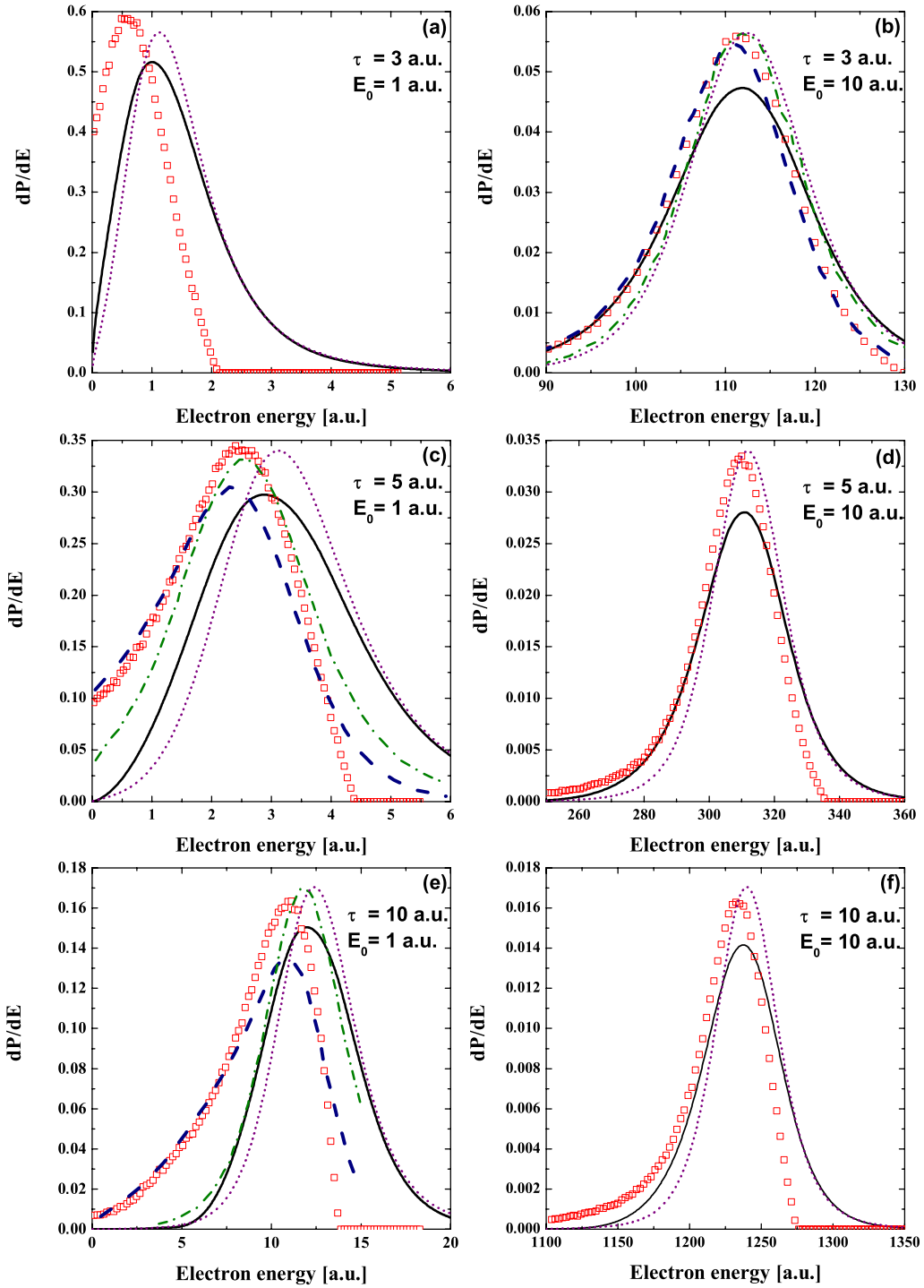

FIG. 5. (Color online) Ionization probability density as function of the electron energy for ω=0.05 a.u. Solid line: MSSFA. Dotted line: Volkov. Squares: CTMC. Dashed line: TDSE [36]. Dash-dotted line: CV [36].

low momentum transfer we found that the Coulomb potential has an important role after the laser pulse is switched off. In the case of longer pulses, with low momentum transfer, the Coulomb potential is equally important during and after the pulse, while in the case of high momentum transfer the Coulomb interaction has a larger influence during the laser pulse.

A good agreement between MSSFA and TDSE (CTMC where TDSE results are not available) results was found at high laser field intensities, where the momentum transfer was high, while at lower intensities with low momentum the agreement was acceptable, comparable with the agreement between the CV and TDSE (CTMC) results. It was shown that except for the case of low momentum transfer, the MSSFA model provides better results than the CV model. The main deficiency of the MSSFA model is that in the case of low momentum transfer the plane waves used for the final

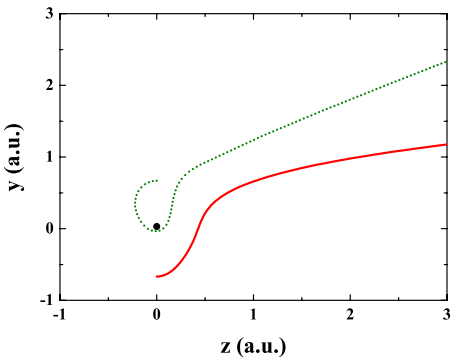

FIG. 6. (Color online) Two possible electron trajectories during the ionization corresponding to photoelectrons with high (solid line) and low (dotted line) ejection energies. The black dot is the residual proton, and the net momentum transfer is along the z axis.

state are inaccurate, which leads to less accurate results. This deficiency can be corrected by using Coulomb wave functions instead of simple plane waves for the final state, which will be the subject of our future investigations.

ACKNOWLEDGMENTS

The work was supported by the Romanian Academy of Sciences (Grant No. 35/3.09.2007), the Romanian National Plan for Research (PN II) under Contract No. ID-539, a grant "Bolyai" from the Hungarian Academy of Sciences, the Hungarian National Office for Research and Technology, and the Hungarian Scientific Research Foundation OTKA (Grant No. K72172).

[1] T. Brabec and F. Krausz, Rev. Mod. Phys. **72**, 545 (2000).
[2] B. Schenkel, J. Biegert, U. Keller, C. Vozzi, M. Nisoli, G. Sansone, S. Stagira, S. De Silvestri, and O. Svelto, Opt. Lett. **28**, 1987 (2003).
[3] M. Y. Shverdin, D. R. Walker, D. D. Yavuz, G. Y. Yin, and S. E. Harris, Phys. Rev. Lett. **94**, 033904 (2005).
[4] P. Agostini, P. Breger, A. L'Huillier, H. G. Muller, G. Petite, A. Antonetti, and A. Migus, Phys. Rev. Lett. **63**, 2208 (1989).
[5] G. G. Paulus, W. Nicklich, H. Xu, P. Lambropoulos, and H. Walter, Phys. Rev. Lett. **72**, 2851 (1994); G. G. Paulus, W. Nicklich, F. Zacher, P. Lambropoulos, and H. Walther, J. Phys. B **29**, L249 (1996).
[6] P. Hansch, M. A. Walker, and L. D. Van Woerkom, Phys. Rev. A **57**, R709 (1998).
[7] M. J. Nandor, M. A. Walker, and L. D. Van Woerkom, J. Phys. B **31**, 4617 (1998).
[8] R. Wiehle, B. Witzel, H. Helm, and E. Cormier, Phys. Rev. A **67**, 063405 (2003).
[9] G. Mainfray and C. Manus, Rep. Prog. Phys. **54**, 1333 (1991).
[10] J. Parker, K. T. Taylor, C. W. Clark, and S. Blodgett-Ford, J. Phys. B **29**, L33 (1996).
[11] M. Protopapas, C. H. Keitel, and P. L. Knight, Rep. Prog. Phys. **60**, 389 (1997).
[12] W. Becker, F. Grasbone, R. Kopold, B. D. Milošević, G. G. Paulus, and H. Walther, Adv. At., Mol., Opt. Phys. **48**, 35 (2002).
[13] R. Radhakrishnan and R. B. Thayyullathil, Phys. Rev. A **69**, 033407 (2004).
[14] B. D. Milošević, G. G. Paulus, D. Bauer, and W. Becker, J. Phys. B **39**, R203 (2006).
[15] A. Rudenko, K. Zrost, C. D. Schröter, V. L. B. de Jesus, B. Feuerstein, R. Moshammer, and J. Ullrich, J. Phys. B **37**, L407 (2004).
[16] C. M. Maharjan, A. S. Alnaser, I. Litvinyuk, P. Ranitovic, and C. L. Cocke, J. Phys. B **39**, 1955 (2006).
[17] G. G. Paulus, F. Grasbon, H. Walter, P. Villoresi, M. Nisoli, S. Stagira, E. Priori, and S. De Silvestri, Nature (London) **414**, 182 (2001).
[18] F. Lindner, M. G. Schätzel, H. Walther, A. Baltuška, E. Goulielmakis, F. Krausz, D. B. Milošević, D. Bauer, W. Becker, and G. G. Paulus, Phys. Rev. Lett. **95**, 040401 (2005).
[19] D. G. Arbó, S. Yoshida, E. Persson, K. I. Dimitriou, and J. Burgdörfer, Phys. Rev. Lett. **96**, 143003 (2006).
[20] E. Cormier and P. Lambropoulos, J. Phys. B **30**, 77 (1997).
[21] H. G. Muller, Phys. Rev. Lett. **83**, 3158 (1999).
[22] H. G. Muller, Laser Phys. **9**, 138 (1999).
[23] Z. Chen, T. Morishita, Anh-Thu Le, M. Wickenhauser, X. M. Tong, and C. D. Lin, Phys. Rev. A **74**, 053405 (2006).
[24] J. P. Hansen, J. Lu, L. B. Madsen, and H. M. Nilsen, Phys. Rev. A **64**, 033418 (2001).
[25] M. Awasthi and A. Saenz, J. Phys. B **39**, S389 (2006).
[26] Xi Chu and Shih-I Chu, Phys. Rev. A **63**, 023411 (2001).
[27] P. Kruit, J. Kimman, H. G. Muller, and M. J. van der Wiel, Phys. Rev. A **28**, 248 (1983).
[28] W. Xiong, F. Yergeau, S. L. Chin, and P. Lavigne, J. Phys. B **21**, L159 (1988).
[29] L. V. Keldysh, Sov. Phys. JETP **20**, 1307 (1965).
[30] H. R. Reiss, Phys. Rev. A **22**, 1786 (1980).
[31] R. R. Freeman, P. H. Bucksbaum, H. Milchberg, S. Darack, D. Schumacher, and M. E. Geusic, Phys. Rev. Lett. **59**, 1092 (1987).
[32] S. Chelkowski and A. D. Bandrauk, Phys. Rev. A **71**, 053815 (2005).
[33] D. M. Wolkow, Z. Phys. **94**, 250 (1935).
[34] V. S. Popov, Phys. Usp. **47**, 855 (2004).
[35] G. Duchateau, E. Cormier, and R. Gayet, Eur. Phys. J. D **11**, 191 (2000).
[36] G. Duchateau, C. Illescas, B. Pons, E. Cormier, and R. Gayet, J. Phys. B **33**, L571 (2000).
[37] G. Duchateau, E. Cormier, and R. Gayet, Phys. Rev. A **66**, 023412 (2002).
[38] R. Gayet, J. Phys. B **38**, 3905 (2005).
[39] M. Jain and N. Tzoar, Phys. Rev. A **18**, 538 (1978).
[40] V. D. Rodríguez, E. Cormier, and R. Gayet, Phys. Rev. A **69**, 053402 (2004).
[41] C. R. Feeler and R. E. Olson, J. Phys. B **33**, 1997 (2000).

[42] Xingdong Mu, Phys. Rev. A **43**, 5149 (1991).
[43] J. Zhang and T. Nakajima, Phys. Rev. A **75**, 043403 (2007).
[44] R. Abrines and I. C. Percival, Proc. Phys. Soc. London **88**, 861 (1966).
[45] R. E. Olson and A. Salop, Phys. Rev. A **16**, 531 (1977).
[46] K. Tőkési and G. Hock, Nucl. Instrum. Methods Phys. Res. B **86**, 201 (1994).